




ARTICLE



<https://doi.org/10.1038/s43247-020-00066-7>

OPEN

Inherited geochemical diversity of 3.4 Ga organic films from the Buck Reef Chert, South Africa

Julien Alleon ^{1✉}, Sylvain Bernard², Nicolas Olivier³, Christophe Thomazo^{4,5} & Johanna Marin-Carbonne¹

Archean rocks contain crucial information about the earliest life forms on Earth, but documenting these early stages of biological evolution remains challenging. The main issue lies in the geochemical transformations experienced by Archean organic matter through its multi-billion-year geological history. Here we present spatially resolved chemical investigations conducted on 3.4 Ga organic films from the Buck Reef Chert, South Africa which indicate that they possess significantly different chemical compositions. Since these organic films all underwent the same post-depositional geological history, this geochemical diversity is most likely inherited, reflecting original chemical differences which were not completely obliterated by subsequent burial-induced degradation processes. These results demonstrate that early Archean organic films carry chemical information directly related to their original molecular compositions. This paves the way for the reconstruction of the initial chemical nature of organic microfossils found in ancient rocks, provided that the geologically-induced chemical transformations they underwent are properly constrained.

¹Institut des sciences de la Terre (ISTE), Université de Lausanne, 1015 Lausanne, Switzerland. ²Muséum National d'Histoire Naturelle, CNRS, Sorbonne Université, Institut de Physique des Matériaux et de Cosmochimie (IMPMC), 75005 Paris, France. ³Université Clermont Auvergne, CNRS, IRD, Laboratoire Magmas et Volcans, 63170 Aubière, France. ⁴Université de Bourgogne Franche-Comté, UMR CNRS 6282 Biogéosciences, 21000 Dijon, France. ⁵Institut Universitaire de France, 75005 Paris, France. ✉email: julien.alleon@gmail.com

The ancient fossil record contains crucial information about the evolution of early life on Earth^{1–3}. Yet, the biogeochemical signals that can be retrieved from ancient rocks are not pristine: multiple alteration processes inevitably modify the chemical composition of organic molecules over geological timescales, which makes it particularly challenging to reconstruct the original chemical nature of Paleoproterozoic organic-rich structures, and thence to distinguish authentic microbial remains from abiotic ones^{4–6}.

Although the general perception in paleobiology has long been that thermal maturation processes lead to a converging composition of organic materials from different origins⁷, several studies have demonstrated that organic molecules may undergo only partial degradation during their geological history^{8–15}. In parallel, laboratory experiments have evidenced that burial-induced thermal degradation processes may not completely obliterate organic geochemical signals^{16–26} and have suggested that initial organic molecular heterogeneities can withstand diagenesis and be recognized in the fossil record²⁷.

Many studies have reported the occurrence of organic films in a number of Paleoproterozoic cherts^{13,15,28–39}. Yet, besides the work of Westall, et al.³² and Alleon, et al.¹³, these studies did not investigate the molecular composition of these microstructures. Here, we report results of spatially resolved elemental and molecular investigations conducted using transmission electron microscopy (TEM) and scanning transmission X-ray microscopy (STXM) on 3.4 Ga organic films from the Buck Reef Chert (BRC, Kaapvaal Craton, South Africa). We interpret the geochemical diversity of the BRC organic films investigated as inherited, i.e., the chemical differences between the films result from initial chemical differences, even though these organic films underwent a significant degradation during their geological history.

Results

Scanning electron microscopy (SEM) observations reveal that the BRC organic films are draped over the microquartz crystals (Fig. 1). Besides slight wrinkles, these films display an overall smooth surface texture, with clear imprints of microquartz crystals. Parts of some of the films are below the freshly exposed surface investigated, i.e., trapped within the microquartz matrix of the sample (see also Supplementary Fig. 1).

According to Raman data, the BRC organic films are rather homogeneous in terms of structural order of their aromatic skeleton. In fact, all these films display similar Raman signals typical of disordered carbonaceous materials, with a rather intense and narrow D1 band and a less intense composite G + D2 band (Fig. 2 and Supplementary Fig. 2). Application of the RSCM (Raman spectroscopy of carbonaceous material) geothermometer⁴⁰ indicates that the organic films were exposed to peak temperature conditions around 300 °C, which is consistent with previous studies of the geological history of the BRC^{41,42}. Assimilated, SEM and Raman spectroscopy testify to the syngenicity of the BRC organic films, i.e., they were trapped within the chert at the time of its formation.

TEM investigations conducted on Focused ion beam (FIB) foils extracted from five BRC organic films (red segments on Films 1–5, Fig. 1) evidence the absence of gap/space between the organic films and the chert matrix, even at the nanometer scale (Fig. 3). Besides the microquartz crystals, no mineral phases can be observed within the FIB foils investigated: the organic films are exclusively composed of carbonaceous compounds (Fig. 3).

Spatially-resolved chemical investigation using STXM reveals that the BRC organic films possess variable N/C values (from 0.05 to 0.16 ± 0.02 ; Fig. 4a), indicating a significant chemical variability among the BRC organic films. The C-X-ray absorption near edge

structure (XANES) spectra (Fig. 4) display multiple absorption features. The large and more or less asymmetrical features centered at about 285.2 eV signal the presence of olefinic/aromatic groups and heterocycles, while the more or less defined peaks/shoulders centered at 286.7 eV reveal the presence of imine (C=N), nitrile (C≡N), carbonyl (C=O) and/or phenolic (Ar-OH) groups^{27,43,44}. The peaks at 289.4 eV signal the presence of hydroxyl (OH) groups while the relatively intense contributions at 288 eV likely reflect the contribution of aliphatic carbons, although a contribution from amide ((R₁, R₂)N-C=O) groups at 288.2 eV cannot be excluded^{27,43,44}. Of note, the relative intensities of these features do not vary within each film (Supplementary Fig. 3) but vary significantly between the films investigated (Fig. 4 and Supplementary Fig. 4), confirming the significant chemical differences between the BRC organic films investigated. In fact, the organic films 1, 2, and 4 contain more heterocycles and O-rich and N-rich functional groups than the organic films 3 and 5, the organic film 3 being richer in aliphatics and hydroxyls than the organic film 5. Differences between the films are less obvious at the N K-edge. Still, the features centered at 401.2 eV, likely related to the presence of amide, imine and/or nitrile groups, are only detected in the organic films 3 and 5, and the contribution of N-rich heterocycles (the peak at 399.9 eV and the shoulder around 398.8 eV^{27,43,45}) is higher for the organic films 1, 2, and 4 than for the organic films 3 and 5. Altogether, despite a similar morphology, the BRC organic films investigated here are not chemically identical.

Discussion

Inherited geochemical diversity. The BRC organic films investigated have experienced only partial degradation despite a long geological history punctuated by episodes of metamorphism in the lower greenschist facies (Fig. 2). The molecular composition of the BRC organic films is not that different, at the first order, from that of organic films found in chert of the 3.4 Ga Strelley Pool Formation¹³. Such preservation, with significant quantities of hydrogen, nitrogen and oxygen retained in the BRC organic films, may be related to their early entombment within silica. In fact, experimental work demonstrated that such early entombment within silica limits the molecular degradation of microorganisms during advanced diagenesis^{21,23}. Early entombment is believed to explain the high level of molecular preservation previously reported for organic microfossils in cherts of the 1.9 Ga Gunflint¹² and the 3.4 Ga Strelley Pool¹³ formations. This study thus exemplifies once again that Archean cherts are pertinent targets for the search for (at least partially) chemically preserved remains of ancient life.

While the BRC organic films are morphologically and texturally similar, they differ significantly from each other in terms of elemental and molecular compositions (Fig. 4). These chemical variations cannot be due to post-depositional mineralogical effects. In fact, although distinct mineral phases will not impact similarly the thermal degradation of organic molecules^{17,21–24,26,46}, the BRC organic films investigated are only associated to microquartz (Figs. 1 and 3). The chemical variability observed here is also difficult to explain by post-depositional processes involving fluid circulation. In fact, because liquid water enhances their reactivity^{47–52}, the circulation of fluids can only be detrimental to the molecular preservation of organic compounds. Yet, there is no organic carbon at microquartz crystal boundaries in the chert matrix which would testify to the infiltration of oil or to the fluid-deposition of organic carbon, in contrast to what was described in the 340 Ma Red Dog Zn-Pb deposit (Alaska)⁵³ or in the 3.5 Ga chert of the Mount Ada Basalt (Pilbara, Australia)⁵⁴.

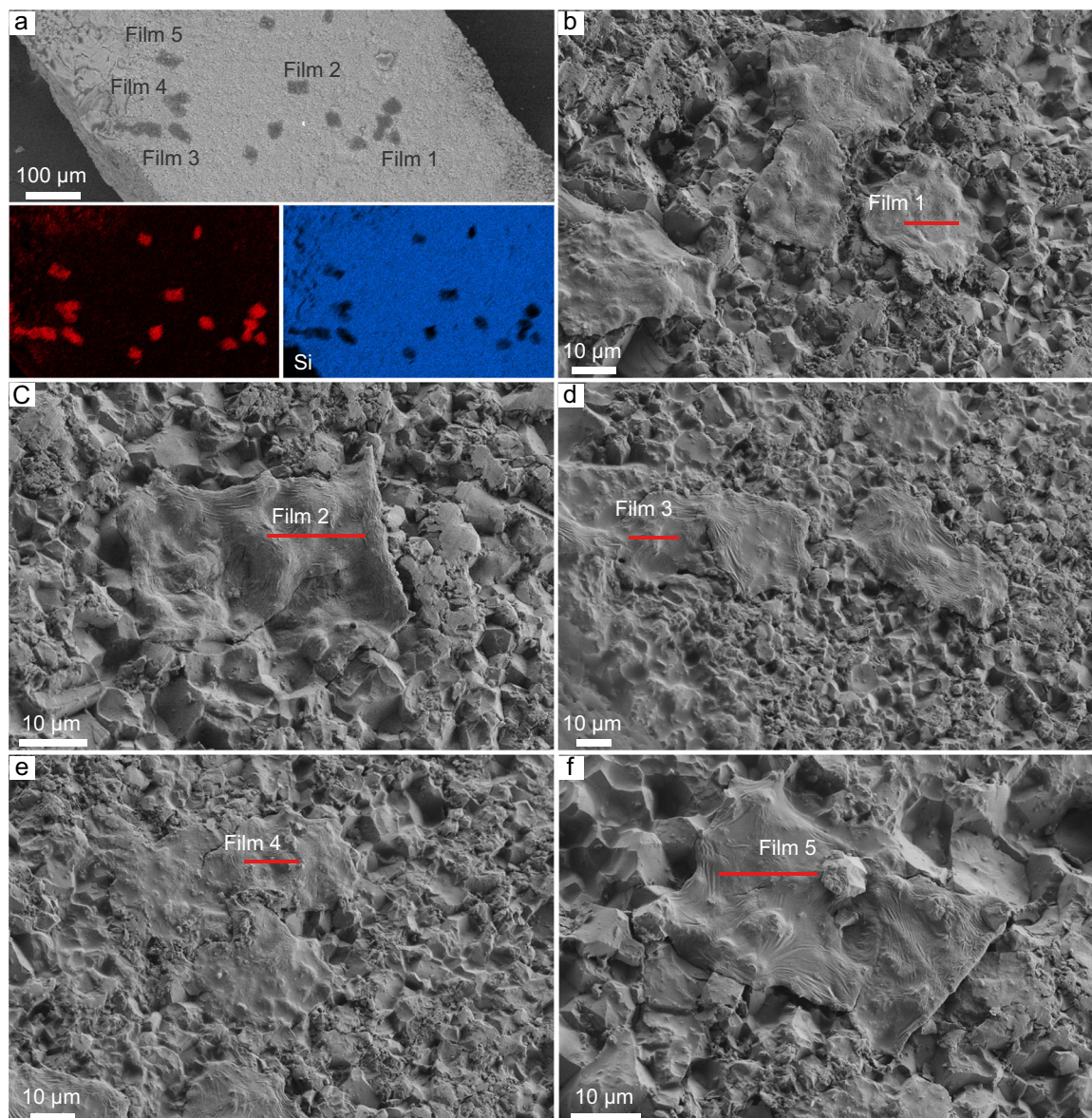


Fig. 1 SEM images of the BRC organic films. **a** SEM [BSE] photomicrograph of a surface of freshly fractured chert, and corresponding EDX maps showing the distribution of carbonaceous films (dark; map 'C') in the chert matrix composed of microquartz (light; map 'Si'); **(b-f)** SEM [SE] photomicrographs of individual films from which FIB foils have been extracted (red segments).

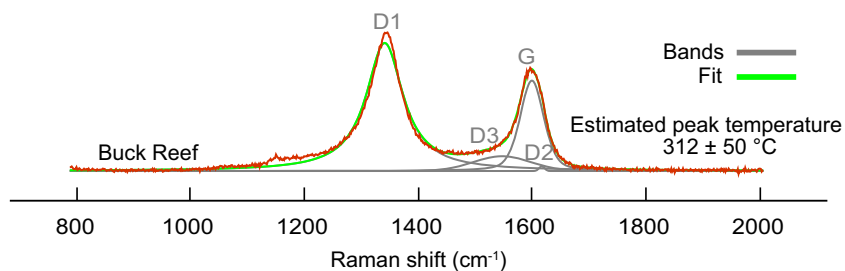


Fig. 2 Raman spectroscopy of the BRC organic films. Representative Raman spectrum of the BRC organic films and its decomposition with a Voigt function. 4 bands were used to decompose the signal and estimate the maximum temperature experienced by carbonaceous matter, following Beysac, et al.⁴⁰.

Rather than a result of post-depositional alteration processes, the chemical variability observed here can be seen as a legacy, i.e., this geochemical diversity is very likely inherited. In other words, the BRC organic films investigated here were initially chemically different and post-depositional degradation

processes did not completely obliterate these differences. This is totally consistent with recent experimental results having suggested/predicted that organic molecular heterogeneities can withstand diagenesis and be recognized in the geological record²⁷.

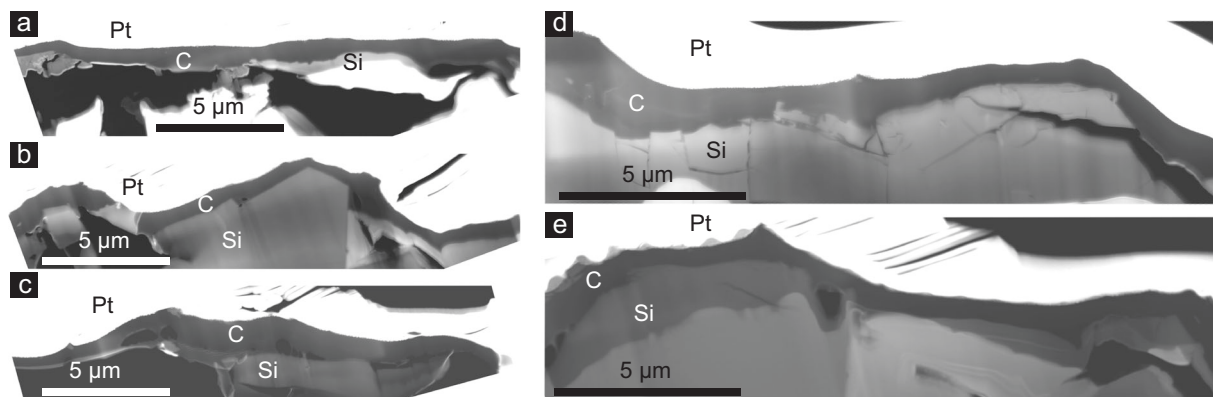


Fig. 3 TEM images of the BRC organic films. STEM images of the FIB foils extracted from 5 BRC organic films (a–e) showing the distribution of carbon (C) and quartz (Si). Pt refers to platinum. Most films are less than one micron thick and are made of pure carbon. Note the close contact between the thin organic films and the chert matrix.

Implications for the origin/nature of the BRC organic films. As is the case of many microstructures found in Paleoproterozoic cherts^{5,6}, determining whether the BRC organic films investigated here are biogenic or abiotic is not straightforward. Carbonaceous laminations and 100 μm -thick films interpreted as fossilized microbial mats were previously reported in the BRC^{29,34,35,37}. Because the organic films investigated here are much smaller, the direct comparison is difficult. Organic films interpreted as fossilized biofilms were previously described in a black chert sample from another unit of the Kromberg Formation³¹ and from the Strelley Pool Formation^{13,15}. In contrast to the BRC organic films investigated here, the Kromberg organic films were reported to be composed of multiple layers of parallel 0.25 μm -thick filaments that are thickly coated with a heterogeneously textured film that ranges from roopy, granular, smooth, to holey³¹, while the Strelley Pool organic films were reported to display surface textures that range from granular to smooth and slightly wrinkled^{13,15}. In addition, contrasting with the BRC organic films investigated here, the Strelley Pool organic films were reported to have broadly similar elemental and molecular compositions, consistent with geologically altered biological compounds, whatever their fine scale texture¹³. It thus appears difficult to interpret the BRC organic films investigated here as being similar in nature to the Kromberg and Strelley Pool organic films.

Even though this would not constitute a biosignature in itself, the absence of amide and carboxylic functional groups in some of the BRC organic films investigated (Fig. 4) makes it difficult to conclude on their biogenicity at this stage. The fact that the BRC organic films were initially chemically different (cf. above) appears consistent with a biogenic origin. In modern stromatolites, extracellular polymeric secretions can indeed display heterogeneous chemical degradation rates, and N-enriched organic residues are produced from the degradation of carbohydrates by heterotrophic microorganisms⁵⁵. Yet, it can be conceived that the BRC organic films investigated here were produced by abiotic processes having occurred prior to the geological history of the BRC. Abiotic processes can indeed lead to the formation of nitrogen-rich organic compounds and chemically heterogeneous kerogen-like particles as those found in carbonaceous chondrites^{56–59}. In addition, abiotic hydrothermal or atmospheric processes on the Archean Earth, may have produced condensed forms of organic matter, as already suggested for some carbonaceous materials of the BRC³⁵. Worse, experimental studies of thermal degradation processes have shown that abiotic organic compounds may produce organic residues difficult to distinguish from remains of biogenic organic compounds^{27,60}, especially given that the thermal degradation of biogenic organic compounds has been shown to be more abstruse

than historically believed^{16–20,22,24–26,46,61–63}. At the end, although they fulfill many (if not all) of the commonly used criteria of biogenicity, even the most conservative ones⁶⁴, further quantitative constraints on the impact of a geological history on biogenic and abiotic organic compounds appear necessary to determine the exact origin of the BRC organic films investigated here.

Concluding remarks. Archean rocks have been exposed to complex geological processes that have caused the degradation of biomolecules and/or abiotic synthesis of organic molecules with chemical features similar to those produced by living organisms^{5,6,65}. Here, we provide compelling evidence that inherited molecular differences can survive a 3.4-billion-year-long geological history punctuated by metamorphic events. Altogether, the present results highlight that ancient organic microstructures still carry information on their initial chemical nature. This initial nature could be reconstructed provided robust experimental constraints on the impact of a geological history on the chemical transformations of organic compounds. Undoubtedly, such reconstructions, associated with detailed chemical characterization such as exemplified in this work, would have major implications for our understanding of early life on Earth and potentially beyond.

Methods

3.4 Ga BRC sample. The BRC is the basal member of the 3.4–3.3 Ga Kromberg Formation of the upper Onverwacht Group in the Kaapvaal Craton, South Africa^{35,66–68}. The BRC consists of silicified evaporites onto which are lying black and white, and banded ferruginous cherts⁶⁹. Silica precipitation occurred directly from seawater on a subsiding volcanic platform^{35,69,70} or resulted from the hydrothermal silicification of volcanoclastic deposits in a shallow water platform^{36,71,72}. For this study, BRC samples of the lower black and white chert were collected in 2017 (25°55′33.6″S, 30° 54′28.8″E; top of the K1e Member). A black chert sample was selected for this study, because Paleoproterozoic organic structures interpreted as fossilized biofilms were previously reported in similar rocks of the same Kromberg Formation^{29,31,34,35,37}. The chert sample investigated here was only mechanically fractured to expose fresh surfaces for further Raman, SEM, TEM, and STXM experiments, as previously done for similar Paleoproterozoic cherts^{12,13,54}, thereby avoiding organic contamination issues related to resin embedding and polishing.

Raman spectroscopy. Raman spectroscopy was used to document the degree of structural organization of the aromatic skeleton of the carbonaceous material composing the films investigated. Raman data were obtained using a Renishaw INVIA spectrometer (IMPMC, Paris, France) in a confocal configuration equipped with a 514.5-nm wavelength 50-mW Modulaser Ar laser, on a surface of freshly fractured chert sample, at room temperature. The configuration used yields a horizontal resolution of $\approx 1 \mu\text{m}$ for a laser power delivered at the sample surface below 1 mW, thereby preventing irreversible thermal damage^{73,74}. Extraction of spectral parameters from peak fitting procedures and estimation of peak

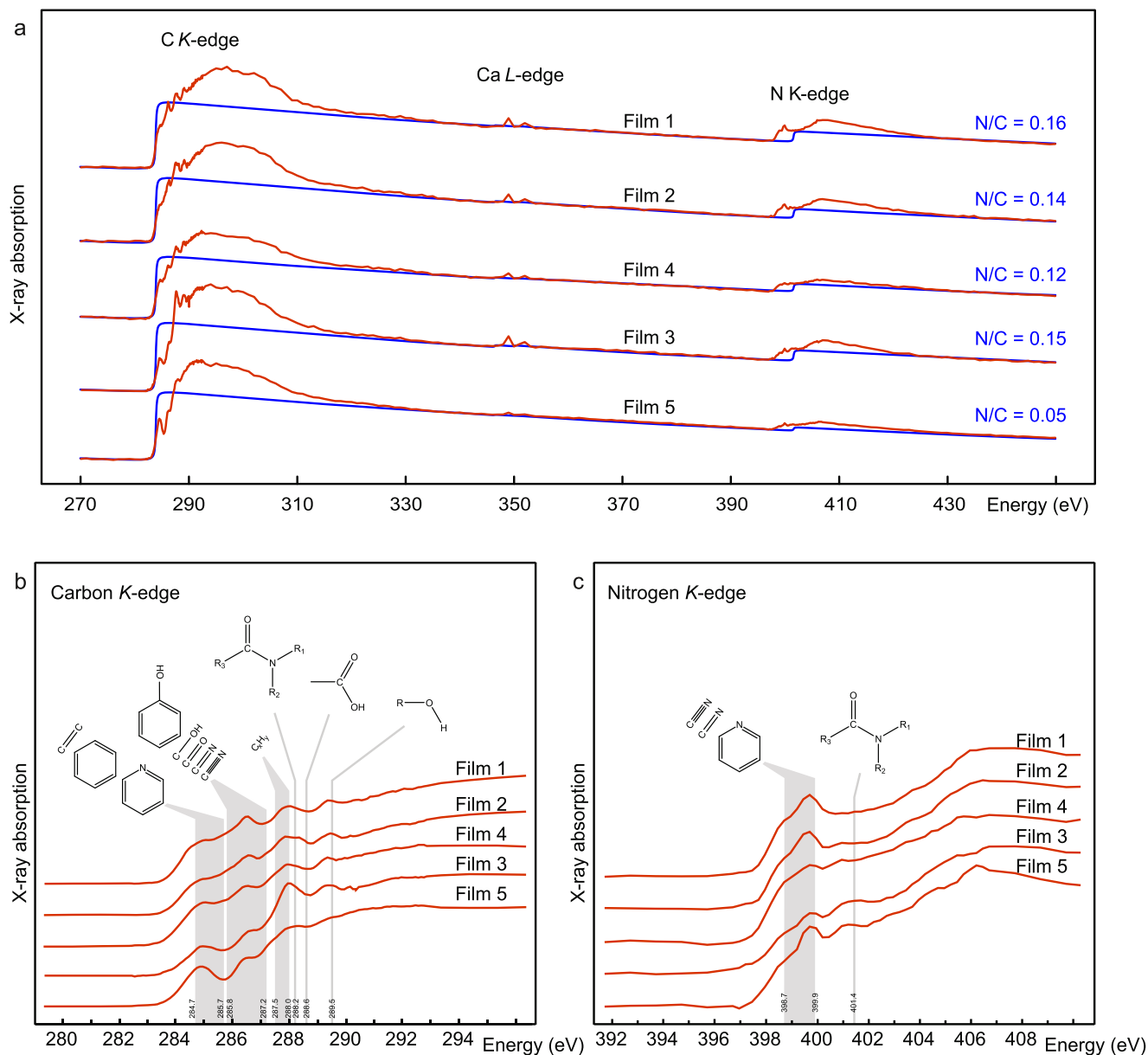


Fig. 4 STXM-based X-ray absorption analyses. **a** X-ray absorption spanning the carbon and nitrogen K-edge energies of the BRC organic films shown in Figs. 1, 3, and their corresponding N/C values. X-ray absorption near edge structure (XANES) spectra at **(b)** the carbon K-edge and **(c)** the nitrogen K-edge. Diagnostic absorption features include: 284.7–285.7 eV for quinone/heterocyclic/aromatic/olefinic groups, 285.8–287.2 eV for imine/nitrile/carbonyl/phenol groups, 287.5–288.0 eV for aliphatic groups, 288.2 eV for amide groups, 288.6 eV for carboxyl/ester/acetal groups, 289.4 eV for hydroxyl groups, 398.8–399.9 eV for imine/nitrile/aromatic groups, 401.4 eV for amide groups.

temperature experienced by organic carbon were done following the methodology described by Beyssac, et al.⁴⁰.

Scanning electron microscopy. SEM was used to document the texture of the organic films measured using Raman before their extraction by FIB milling. Chert fragments analyzed with Raman were mounted on aluminum stubs without any additional preparation, except Pt coating. SEM observations were performed with a SEM–field emission gun ultra 55 Zeiss (IMPMC, Paris, France) at 2 and 10-kV accelerating voltage for secondary and back-scattered electron analyses, respectively.

Focused ion beam. FIB foils were extracted for TEM and STXM investigations using a FEI Strata DB 235 (IEMN, Lille, France). Milling at low Ga-ion currents allowed minimizing artefacts such as gallium implantation, amorphization, composition changes or redeposition of the sputtered material^{75,76}.

Transmission electron microscopy. TEM analyses were performed on FIB foils to document, down to the nanoscale, the texture and relationships between

microquartz and the organic materials composing the films investigated. TEM observations were conducted with a JEOL 2100 field emission gun microscope (IMPMC, Paris, France) operating at 200 kV. Z-contrast STEM imaging was performed using the high-angle annular dark field mode.

STXM coupled with XANES spectroscopy. STXM-based XANES spectroscopy analyses were performed on FIB foils to document both the carbon and nitrogen speciation and the N/C values of the films investigated using the HERMES STXM beamline at the synchrotron SOLEIL (Saint-Aubin, France)^{77,78}. Energy calibration was done using the well-resolved 3p Rydberg peak of gaseous CO₂ at 294.96 eV for the C K-edge, and using the 1 → π* photoabsorption resonance of gaseous N₂ at 400.8 eV for the N K-edge. XANES hypercube data (stacks) were collected with a spatial resolution of 35 nm at energy increments of 1 eV over the 250–450 eV region and at energy increments of 0.1 eV over the carbon (270–340 eV) and the nitrogen (390–450 eV) K-edges with a dwell time of less than 1 ms per pixel to prevent irradiation damage⁷⁹. Stack alignment and extraction of XANES spectra were done using the aXis2000 software (ver2.1n). The XANES spectra shown here are the sum of hundreds of spectra collected over homogeneous organic-rich areas

of several hundreds of square nanometers. N/C atomic ratio values and quantitative spectral parameters were estimated using both the methodology outlined by Alleon, et al.⁸⁰ and using the QUANTORXS freeware⁴⁴.

Data availability

The data supporting the findings of this study are available on Zenodo (<https://doi.org/10.5281/zenodo.4015138>). The samples are available from the corresponding author (J.A.) upon request.

Received: 23 June 2020; Accepted: 20 November 2020;

Published online: 04 January 2021

References

- Brasier, M. D., Antcliffe, J., Saunders, M. & Wacey, D. Changing the picture of Earth's earliest fossils (3.5–1.9 Ga) with new approaches and new discoveries. *Proc. Natl Acad. Sci. USA* **112**, 4859–4864 (2015).
- Javaux, E. J. & Lepot, K. The Paleoproterozoic fossil record: implications for the evolution of the biosphere during Earth's middle-age. *Earth-Sci. Rev.* **176**, 68–86 (2018).
- Lepot, K. Signatures of early microbial life from the Archean (4 to 2.5 Ga) eon. *Earth-Sci. Rev.* **209**, 103296 (2020).
- Bernard, S. & Papineau, D. Graphitic carbons and biosignatures. *Elements* **10**, 435–440 (2014).
- Alleon, J. & Summons, R. E. Organic geochemical approaches to understanding early life. *Free Radical Biol. Med.* **140**, 103–112 (2019).
- Javaux, E. J. Challenges in evidencing the earliest traces of life. *Nature* **572**, 451–460 (2019).
- Briggs, D. E. G. & McMahon, S. The role of experiments in investigating the taphonomy of exceptional preservation. *Palaeontology* **59**, 1–11 (2016).
- Bernard, S. et al. Exceptional preservation of fossil plant spores in high-pressure metamorphic rocks. *Earth Planet. Sci. Lett.* **262**, 257–272 (2007).
- Bernard, S., Benzerara, K., Beyssac, O. & Brown, G. E. Multiscale characterization of pyritized plant tissues in blueschist facies metamorphic rocks. *Geochim. Cosmochim. Acta* **74**, 5054–5068 (2010).
- Cody, G. D. et al. Molecular signature of chitin-protein complex in Paleozoic arthropods. *Geology* **39**, 255–258 (2011).
- Ehrlich, H. et al. Discovery of 505-million-year old chitin in the basal demosponge *Vauxia gracilenta*. *Sci. Rep.* **3**, 1–6 (2013).
- Alleon, J. et al. Molecular preservation of 1.88 Ga Gunflint organic microfossils as a function of temperature and mineralogy. *Nat. Commun.* **7**, 11977 (2016).
- Alleon, J. et al. Chemical nature of the 3.4 Ga Strelley Pool microfossils. *Geochem. Perspect. Lett.* **7**, 37–42 (2018).
- Loron, C. C. et al. Early fungi from the Proterozoic era in Arctic Canada. *Nature* **570**, 232–235 (2019).
- Delarue, F. et al. Out of rock: A new look at the morphological and geochemical preservation of microfossils from the 3.46 Gyr-old Strelley Pool Formation. *Precambrian Res.* **336**, 105472 (2020).
- Schiffbauer, J. D. et al. Thermally-induced structural and chemical alteration of organic-walled microfossils: an experimental approach to understanding fossil preservation in metasediments. *Geobiology* **10**, 402–423 (2012).
- Li, J. et al. Impact of biomineralization on the preservation of microorganisms during fossilization: an experimental perspective. *Earth Planet. Sci. Lett.* **400**, 113–122 (2014).
- Bernard, S., Benzerara, K., Beyssac, O., Balan, E. & Brown, G. Jr Evolution of the macromolecular structure of sporopollenin during thermal degradation. *Heliyon* **1**, e00034 (2015).
- Colleary, C. et al. Chemical, experimental, and morphological evidence for diagenetically altered melanin in exceptionally preserved fossils. *Proc. Natl Acad. Sci.* **112**, 12592–12597 (2015).
- Picard, A., Kappler, A., Schmid, G., Quaroni, L. & Obst, M. Experimental diagenesis of organo-mineral structures formed by microaerophilic Fe (II)-oxidizing bacteria. *Nat. Commun.* **6**, 6277 (2015).
- Alleon, J. et al. Early entombment within silica minimizes the molecular degradation of microorganisms during advanced diagenesis. *Chem. Geol.* **437**, 98–108 (2016).
- Miot, J., Bernard, S., Bourreau, M., Guyot, F. & Kish, A. Experimental maturation of Archaea encrusted by Fe-phosphates. *Sci. Rep.* **7**, 16984 (2017).
- Igisu, M. et al. Changes of aliphatic C–H bonds in cyanobacteria during experimental thermal maturation in the presence or absence of silica as evaluated by FTIR microspectroscopy. *Geobiology* **16**, 412–428 (2018).
- Jacquemot, P. et al. The degradation of organic compounds impacts the crystallization of clay minerals and vice versa. *Sci. Rep.* **9**, 1–6 (2019).
- Viennet, J.-C. et al. Influence of the nature of the gas phase on the degradation of RNA during fossilization processes. *Appl. Clay Sci.* **191**, 105616 (2020).
- Viennet, J.-C. et al. Experimental clues for detecting biosignatures on Mars. *Geochem. Perspect. Lett.* **12**, 28–33 (2019).
- Alleon, J. et al. Organic molecular heterogeneities can withstand diagenesis. *Sci. Rep.* **7**, 1508 (2017).
- Walsh, M. M. Microfossils and possible microfossils from the early archaean onverwacht group, Barberton mountain land, South Africa. *Precambrian Res.* **54**, 271–293 (1992).
- Walsh, M. M. & Lowe, D. R. Modes of accumulation of carbonaceous matter in the early Archean: a petrographic and geochemical study of the carbonaceous cherts of the Swaziland Supergroup. *Geol. Soc. Am.* **329**, 115–132 (1999).
- Westall, F. et al. Early Archean fossil bacteria and biofilms in hydrothermally-influenced sediments from the Barberton greenstone belt, South Africa. *Precambrian Res.* **106**, 93–116 (2001).
- Westall, F. et al. Implications of a 3.472–3.333 Gyr-old subaerial microbial mat from the Barberton greenstone belt, South Africa for the UV environmental conditions on the early Earth. *Philos. Trans. R Soc. London B* **361**, 1857–1876 (2006).
- Westall, F. et al. Implications of in situ calcification for photosynthesis in a ~3.3 Ga-old microbial biofilm from the Barberton greenstone belt, South Africa. *Earth Planet. Sci. Lett.* **310**, 468–479 (2011).
- Westall, F. et al. Archean (3.33 Ga) microbe-sediment systems were diverse and flourished in a hydrothermal context. *Geology* **43**, 615–618 (2015).
- Tice, M. M. & Lowe, D. R. Photosynthetic microbial mats in the 3,416-Myr-old ocean. *Nature* **431**, 549 (2004).
- Tice, M. M. & Lowe, D. R. The origin of carbonaceous matter in pre-3.0 Ga greenstone terrains: a review and new evidence from the 3.42 Ga Buck Reef Chert. *Earth-Sci. Rev.* **76**, 259–300 (2006).
- Hofmann, A. & Bolhar, R. Carbonaceous cherts in the Barberton Greenstone Belt and their significance for the study of early life in the Archean record. *Astrobiology* **7**, 355–388 (2007).
- Tice, M. M., Thornton, D. C. O., Pope, M. C., Olszewski, T. D. & Gong, J. Archean microbial mat communities. *Ann. Rev. Earth Planetary Sci.* **39**, 297–319 (2011).
- Wacey, D., Noffke, N., Saunders, M., Guagliardo, P. & Pyle, D. M. Volcanogenic pseudo-fossils from the ~3.48 Ga dresser formation, Pilbara, Western Australia. *Astrobiology* **18**, 539–555 (2018).
- Hickman-Lewis, K., Cavalazzi, B., Foucher, F. & Westall, F. Most ancient evidence for life in the Barberton greenstone belt: Microbial mats and biofabrics of the ~3.47 Ga Middle Marker horizon. *Precambrian Res.* **312**, 45–67 (2018).
- Beyssac, O., Goffé, B., Chopin, C. & Rouzaud, J.-N. Raman spectra of carbonaceous material in metasediments: a new geothermometer. *J. Metamorph. Geol.* **20**, 859–871 (2002).
- Tice, M. M., Bostick, B. C. & Lowe, D. R. Thermal history of the 3.5–3.2 Ga Onverwacht and Fig Tree Groups, Barberton greenstone belt, South Africa, inferred by Raman microspectroscopy of carbonaceous material. *Geology* **32**, 37–40 (2004).
- van Zuilen, M. A., Chausson, M., Rollion-Bard, C. & Marty, B. Carbonaceous cherts of the Barberton Greenstone Belt, South Africa: isotopic, chemical and structural characteristics of individual microstructures. *Geochim. Cosmochim. Acta* **71**, 655–669 (2007).
- De Gregorio, B. T., Sharp, T. G., Rushdi, A. I. & Simoneit, B. R. *Earliest Life on Earth: Habitats, Environments and Methods of Detection*. 239–289 (Springer, 2011).
- Le Guillou, C., Bernard, S., De la Pena, F. & Le Brech, Y. XANES-based quantification of carbon functional group concentrations. *Anal. Chem.* **90**, 8379–8386 (2018).
- Leinweber, P. et al. Nitrogen K-edge XANES—an overview of reference compounds used to identify unknown organic nitrogen in environmental samples. *J. Synchr. Radiat.* **14**, 500–511 (2007).
- Picard, A., Obst, M., Schmid, G., Zeitvogel, F. & Kappler, A. Limited influence of Si on the preservation of Fe mineral-encrusted microbial cells during experimental diagenesis. *Geobiology* **14**, 276–292 (2015).
- Lewan, M. D. Experiments on the role of water in petroleum formation. *Geochim. Cosmochim. Acta* **61**, 3691–3723 (1997).
- McCollom, T. M., Seewald, J. S. & Simoneit, B. R. T. Reactivity of monocyclic aromatic compounds under hydrothermal conditions. *Geochim. Cosmochim. Acta* **65**, 455–468 (2001).
- Pan, C., Geng, A., Zhong, N., Liu, J. & Yu, L. Kerogen pyrolysis in the presence and absence of water and minerals: Amounts and compositions of bitumen and liquid hydrocarbons. *Fuel* **88**, 909–919 (2009).
- Lewan, M. D. & Roy, S. Role of water in hydrocarbon generation from Type-I kerogen in Mahogany oil shale of the Green River Formation. *Org. Geochem.* **42**, 31–41 (2011).
- Foustoukos, D. I. & Stern, J. C. Oxidation pathways for formic acid under low temperature hydrothermal conditions: Implications for the chemical and

- isotopic evolution of organics on Mars. *Geochim. Cosmochim. Acta* **76**, 14–28 (2012).
52. Bernard, S. & Horsfield, B. Thermal maturation of gas shale systems. *Annu. Rev. Earth Planet. Sci.* **42**, 635–651 (2014).
 53. Rasmussen, B. & Muhling, J. R. Organic-rich microfossils produced by oil infiltration of hollow silicified bacteria: Evidence from the ca. 340 Ma Red Dog Zn-Pb deposit, Alaska. *Geology* **47**, 1107–1111 (2019).
 54. Alleon, J. et al. Organo-mineral associations in chert of the 3.5 Ga Mount Ada Basalt raise questions about the origin of organic matter in Paleoproterozoic hydrothermally influenced sediments. *Sci. Rep.* **9**, 1–13 (2019).
 55. Decho, A. W., Visscher, P. T. & Reid, R. P. Production and cycling of natural microbial exopolymers (EPS) within a marine stromatolite. *Palaeogeogr. Palaeoclimatol. Palaeoecol.* **219**, 71–86 (2005).
 56. Pizzarello, S. & Shock, E. The organic composition of carbonaceous meteorites: the evolutionary story ahead of biochemistry. *Cold Spring Harbor Perspect. Biol.* **2**, a002105 (2010).
 57. Le Guillou, C., Bernard, S., Brearley, A. J. & Remusat, L. Evolution of organic matter in Orgueil, Murchison and Renazzo during parent body aqueous alteration: in situ investigations. *Geochim. Cosmochim. Acta* **131**, 368–392 (2014).
 58. Vinogradoff, V. et al. Paris vs. Murchison: Impact of hydrothermal alteration on organic matter in CM chondrites. *Geochim. Cosmochim. Acta* **212**, 234–252 (2017).
 59. Changela, H. G., Le Guillou, C., Bernard, S. & Brearley, A. J. Hydrothermal evolution of the morphology, molecular composition, and distribution of organic matter in CR (Renazzo-type) chondrites. *Meteorit. Planet. Sci.* **53**, 1006–1029 (2018).
 60. De Gregorio, B. T., Sharp, T. G., Flynn, G. J., Wirick, S. & Hergig, R. L. Biogenic origin for Earth's oldest putative microfossils. *Geology* **37**, 631–634 (2009).
 61. Watson, J. S., Fraser, W. T. & Sephton, M. A. Formation of a polyalkyl macromolecule from the hydrolysable component within sporopollenin during heating/pyrolysis experiments with Lycopodium spores. *J. Anal. Appl. Pyrolysis* **95**, 138–144 (2012).
 62. McNamara, M. E. et al. The fossil record of insect color illuminated by maturation experiments. *Geology* **41**, 487–490 (2013).
 63. McNamara, M. E., Briggs, D. E. G., Orr, P. J., Field, D. J. & Wang, Z. Experimental maturation of feathers: implications for reconstructions of fossil feather colour. *Biol. Lett.* **9**, 20130184 (2013).
 64. Brasier, M. D., Green, O. R. & McLoughlin, N. Characterization and critical testing of potential microfossils from the early Earth: the Apex microfossil debate and its lessons for Mars sample return. *Int. J. Astrobiol.* **3**, 139–150 (2004).
 65. Bernard, S., Criouet, I. & Alleon, J. Recognizing Archean traces of life: difficulties and perspectives. *Encyclopedia of Geology*, 2e. B978-0-08-102908-4.00184-3. (Elsevier, 2020).
 66. Byerly, G. R., Kröner, A., Lowe, D. R., Todt, W. & Walsh, M. M. Prolonged magmatism and time constraints for sediment deposition in the early Archean Barberton greenstone belt: evidence from the Upper Onverwacht and Fig Tree groups. *Precambrian Res.* **78**, 125–138 (1996).
 67. Lowe, D. R. & Byerly, G. R. Stratigraphy of the west-central part of the Barberton Greenstone Belt, South Africa. *Geol. Soc. Am.* **329**, 1–36 (1999).
 68. Hofmann, A., Bolhar, R., Orberger, B. & Foucher, F. Cherts of the Barberton Greenstone Belt, South Africa: petrology and trace-element geochemistry of 3.5 to 3.3 Ga old silicified volcanoclastic sediments. *S. Afr. J. Geol.* **116**, 297–322 (2013).
 69. Lowe, D. R. & Byerly, G. R. An overview of the geology of the barberton greenstone belt and vicinity: implications for early crustal development. *Dev. Precambrian Geol.* **15**, 481–526 (2007).
 70. Ledevin, M., Arndt, N., Chauvel, C., Jaillard, E. & Simionovici, A. The sedimentary origin of black and white Banded Cherts of the Buck Reef, Barberton, South Africa. *Geosciences* **9**, 424 (2019).
 71. de Vries, S. T. & Touret, J. L. Early archaean hydrothermal fluids; a study of inclusions from the ~3.4 Ga Buck Ridge chert, Barberton Greenstone Belt, South Africa. *Chem. Geol.* **237**, 289–302 (2007).
 72. de Vries, S. T., Nijman, W. & de Boer, P. L. Sedimentary geology of the Palaeoproterozoic Buck Ridge (South Africa) and Kittys Gap (Western Australia) volcano-sedimentary complexes. *Precambrian Res.* **183**, 749–769 (2010).
 73. Beyssac, O. et al. On the characterization of disordered and heterogeneous carbonaceous materials by Raman spectroscopy. *Spectrochim. Acta Part A* **59**, 2267–2276 (2003).
 74. Bernard, S., Beyssac, O. & Benzerara, K. Raman mapping using advanced line-scanning systems: geological applications. *Appl. Spectrosc.* **62**, 1180–1188 (2008).
 75. Bernard, S. et al. Ultrastructural and chemical study of modern and fossil sporoderms by Scanning Transmission X-ray Microscopy (STXM). *Rev. Palaeobot. Palynol.* **156**, 248–261 (2009).
 76. Schiffbauer, J. D. & Xiao, S. Novel application of focused ion beam electron microscopy (FIB-EM) in preparation and analysis of microfossil ultrastructures: A new view of complexity in early Eukaryotic organisms. *Palaios* **24**, 616–626 (2009).
 77. Belkhou, R. et al. HERMES: a soft X-ray beamline dedicated to X-ray microscopy. *J. Synchrotron Radiation* **22**, 968–979 (2015).
 78. Swaraj, S. et al. *Journal of Physics: Conference Series*. 012046 (IOP Publishing).
 79. Wang, J. et al. Radiation damage in soft X-ray microscopy. *J. Electron Spectrosc. Related Phenomen.* **170**, 25–36 (2009).
 80. Alleon, J., Bernard, S., Remusat, L. & Robert, F. Estimation of nitrogen-to-carbon ratios of organics and carbon materials at the submicrometer scale. *Carbon* **84**, 290–298 (2015).

Acknowledgements

This research was supported by the European Union's Horizon H2020 research and innovation program ERC (STROMATA, grant agreement 759289; PI Johanna Marin-Carbonne) and by the Laboratory of Excellence ClerVolc. Special thanks go to Mpumalanga Tourism and Parks Agency, especially Mr. Johan Eksteen and Sappi Forest Products, which allowed us access to lands, to Jean-Francois Moyon and Robert Moritz for their assistance during field work, to Olivier Beyssac for his help with Raman spectroscopy, to David Troadec for the preparation of the FIB foils investigated, to Imene Esteve for her expert support with the FEG SEM at IMPMC, to Jean Michel Guigner for his expert support with the FEG TEM at IMPMC, and to Stefan Stanescu and Sufal Swaraj for their expert support with the HERMES STXM beamline at SOLEIL. The SEM facility at IMPMC is supported by Region Ile de France grant SESAME Number I-07-593/R, INSU-CNRS, INP-CNRS and UPMC-Paris 6, and by the Agence Nationale de la Recherche (ANR) grant number ANR-07-BLAN-0124-01. The HERMES beamline (SOLEIL) is supported by the CNRS, the CEA, the Region Ile de France, the Departmental Council of Essonne and the Region Centre.

Author contributions

J.A., S.B., and J.M.-C. conceived and designed the research; All authors contributed to field work and sampling; S.B. performed the Raman and SEM/TEM experiments; J.A. and S.B. performed the STXM-based XANES spectroscopy experiments; J.A. and S.B. interpreted the data and wrote the present article, with critical inputs from N.O., C.T., and J.M.-C.

Competing interests

The authors declare no competing interests.

Additional information

Supplementary information is available for this paper at <https://doi.org/10.1038/s43247-020-00066-7>.

Correspondence and requests for materials should be addressed to J.A.

Peer review information Primary handling editors: Mojtaba Fakhraee, Joe Aslin

Reprints and permission information is available at <http://www.nature.com/reprints>

Publisher's note Springer Nature remains neutral with regard to jurisdictional claims in published maps and institutional affiliations.



Open Access This article is licensed under a Creative Commons Attribution 4.0 International License, which permits use, sharing, adaptation, distribution and reproduction in any medium or format, as long as you give appropriate credit to the original author(s) and the source, provide a link to the Creative Commons license, and indicate if changes were made. The images or other third party material in this article are included in the article's Creative Commons license, unless indicated otherwise in a credit line to the material. If material is not included in the article's Creative Commons license and your intended use is not permitted by statutory regulation or exceeds the permitted use, you will need to obtain permission directly from the copyright holder. To view a copy of this license, visit <http://creativecommons.org/licenses/by/4.0/>.

© The Author(s) 2021